Differentiable Beamforming for Ultrasound Autofocusing

Walter Simson, Louise Zhuang, Sergio J. Sanabria, Neha Antil, Jeremy J. Dahl, Dongwoon Hyun

Stanford University, Stanford, CA 94305 USA

Motivation

- Most, if not all clinical ultrasound scanners assume a constant sound speed.
- Local sound speed variations in the tissue cause phase aberrations, leading to a loss of image focus, geometric distortions, and reduced diagnostic efficacy.
- Estimated local sound speeds can be used to correct phase aberration and has the potential to be a key diagnostic biomarker.

Contributions

- We present **differentiable beamforming for ultrasound autofocusing (DBUA),** a physics-based framework for the rapid quantitative estimation of sound speed and phase aberration correction in heterogeneous tissue.
- We introduce common mid-point phase error from statistical and Fourier optics as a focusing criterion for pulse-echo sound speed estimation.
- DBUA optimizes the common mid-point phase error by differentiating through ultrasound beamforming of sub-apertures and updating sound speed maps via gradient descent.
- DBUA corrects phase aberration in both simulation and *in vivo* settings while simultaneously providing quantitative sound speed maps that can be used for diagnostics (e.g., NAFLD).

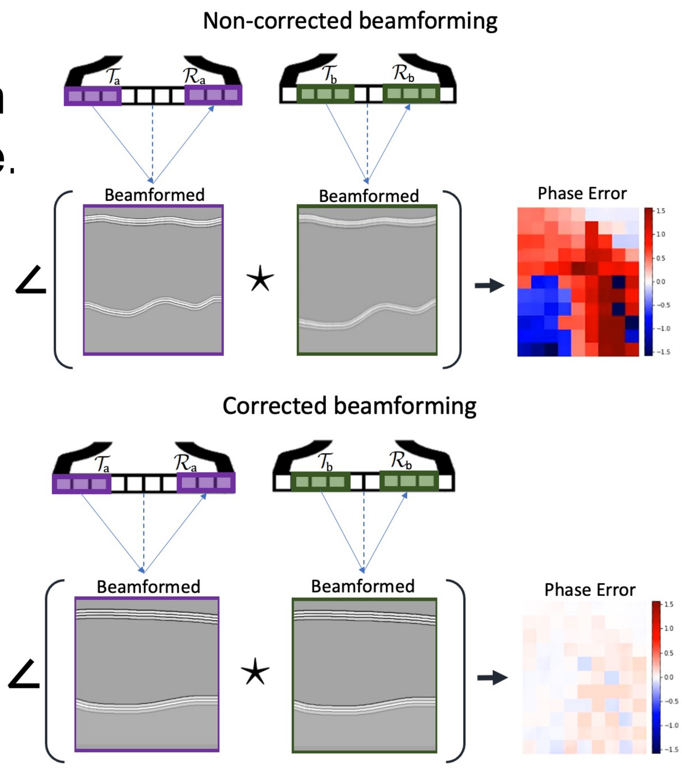

Method

- Beamforming encompasses the process of digitally focusing a received radio-frequency (RF) signal u recorded on a phased array by sampling at a delayed time τ and coherently compounding the sampled signals.

$$u_{ij}(x_k) = u_{ij}\left(\tau(x_i, x_k) + \tau(x_k, x_j)\right) \qquad u(x_k) = \sum_{i=1}^{N_t}\sum_{j=1}^{N_r} u_{ij}(x_k)$$

- Numerically differentiating beamforming via auto-differentiation is possible with modern numerical libraries, which are often used in deep learning applications.
- We investigate the optimization of a slowness map s (inverse of sound speed) given an image quality metric.

$$\mathrm{s}^* = \arg\min_{\mathrm{s}} \mathcal{L}(u(\mathrm{x}_k;\mathrm{s})), \qquad \Delta\mathrm{s} = \mathrm{s} - \alpha\frac{\partial}{\partial \mathrm{s}}\mathcal{L}(u(\mathbf{x}_k;\mathrm{s}))$$

- We explore the metrics of **speckle brightness**, **coherence factor,** and **phase error** of common mid-point sub-aperture pairs.

$$\mathrm{SB}(\mathbf{s}) = \frac{1}{N_k}\sum_k |u(\mathbf{x}_k;\mathbf{s})| = -\mathcal{L}_{\mathrm{SB}}(\mathbf{s}) \qquad \mathrm{CF}(\mathbf{s}) = \frac{1}{N_k}\sum_{k=1}^{N_k}\frac{\left|\sum_j \sum_i u_{ij}(\mathbf{x}_k;\mathbf{s})\right|}{\sum_j \left|\sum_i u_{ij}(\mathbf{x}_k;\mathbf{s})\right|} = -\mathcal{L}_{\mathrm{CF}}(\mathbf{s})$$

$$\Delta\phi_{ab}(\mathbf{x_k}) = \angle\mathbb{E}[u_a(\mathbf{x_k};\mathbf{s})u_b^*(\mathbf{x_k};\mathbf{s})] \qquad \mathrm{PE}(\mathbf{s}) = \frac{1}{N_{(a,b)}}\sum_{(a,b)}|\Delta\phi_{ab}| = \mathcal{L}_{\mathrm{PE}}(\mathbf{s})$$

Proposed

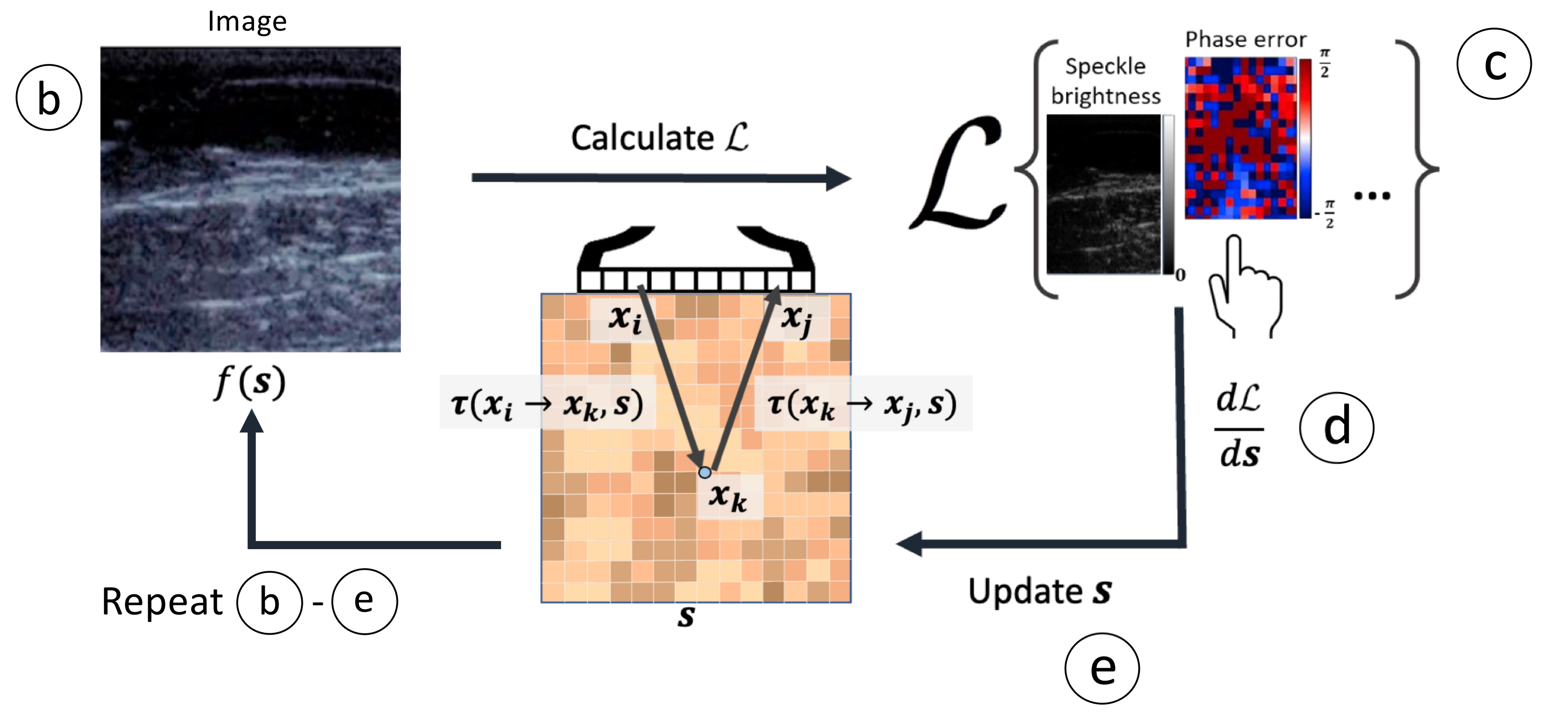

a. Full-synthetic aperture acquisition
b. Delay calculation with straight ray integration and beamforming
c. Calculation of objective function
d. Backpropagation through beamforming to slowness map
e. Update of sound speed map
f. Continue from step b.

Results

- We show that DBUA corrects errors due to aberration while generating quantitative sound speed maps.
- DBUA displays increased resolution when compared to state-of-the-art sound speed reconstruction method CUTE [1].
- DBUA shows promising results on *in vivo* liver data. DBUA resolves fat and abdominal layers.
- DBUA with phase error leads to the lowest quantitative error value in heterogenous phantoms.

Phantom	Description	CUTE (baseline)	Speckle Brightness	Coherence Factor	Phase Error (proposed)
1420	homogenous	21.6±21.4	3.9±3.3	**3.2±2.6**	4.8±3.5
1465	homogenous	11.7±18.8	4.5±4.9	5.3±4.6	**4.5±3.5**
1480	homogenous	10.4±18.5	6.1±5.4	**4.1±4.2**	4.7±3.5
1510	homogenous	10.8±17.0	6.1±7.0	**4.4±4.5**	4.8±3.6
1540	homogenous	11.8±15.8	7.8±7.5	**5.1±4.4**	6.1±4.3
1555	homogenous	11.4±15.3	**5.7±6.7**	5.8±4.7	5.9±4.3
1570	homogenous	11.2±14.8	7.5±7.6	**4.9±4.7**	6.5±4.7
Quadrant	Fig.3a	65.6±36.3	63.2±52.1	63.4±47.7	**35.4±27.9**
Two layer	[17]	40.2±34.1	62.5±54.2	33.2±25.8	**13.4±14.7**
Four layer	[17]	44.1±27.5	50.5±25.0	43.8±23.2	**29.0±26.5**
Inclusion	[17]	14.3±16.4	8.3±7.5	7.5±5.9	**6.1±4.4**
Inclusion layer	[17], Fig.3b	19.8±18.1	16.3±14.8	15.0±11.1	**7.5±5.0**

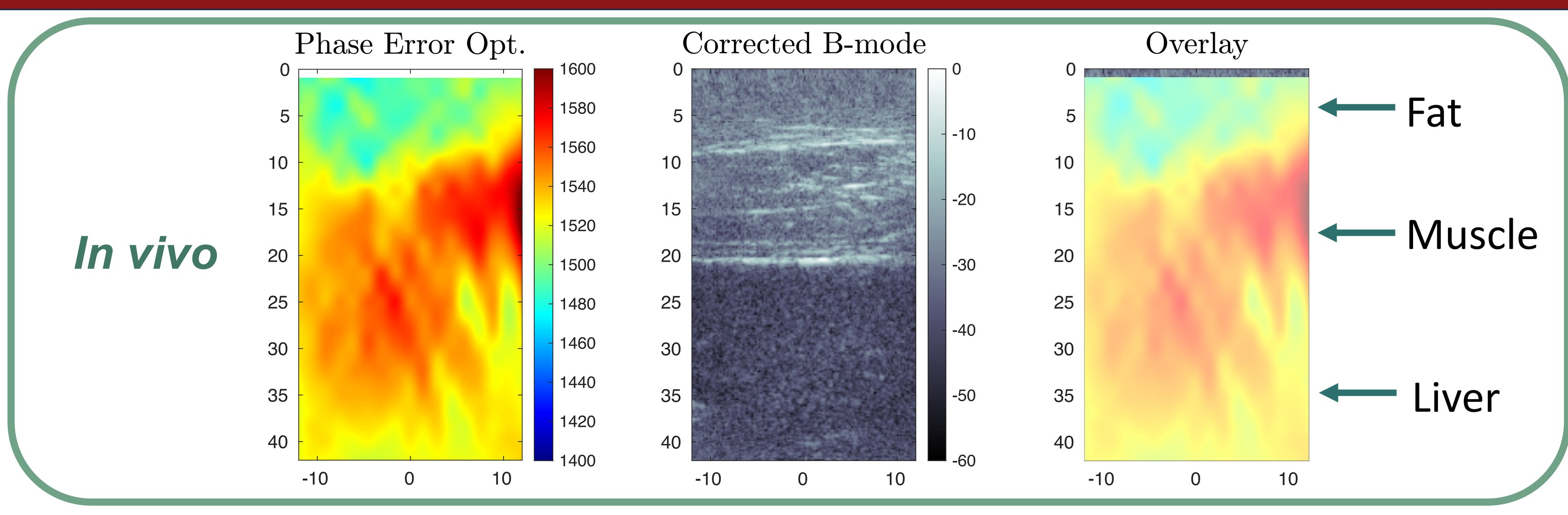

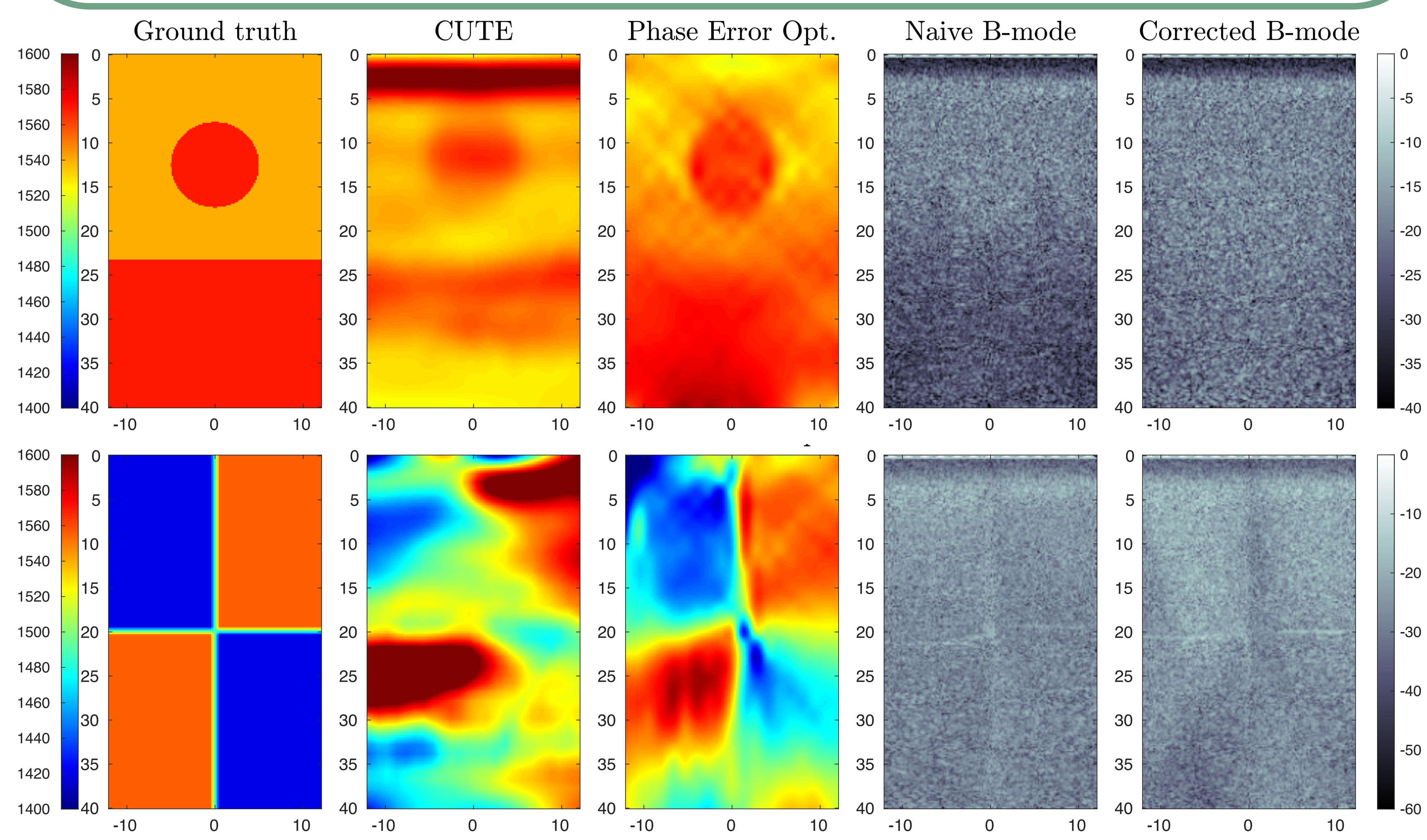

[1] Stähli, P., Kuriakose, M., Frenz, M. and Jaeger, M., 2020. Improved forward model for quantitative pulse-echo speed-of-sound imaging. *Ultrasonics*, *108*, p.106168.